Hydrogen embrittlement
of a medium carbon Q&P steel

G. Lovicu, E. Paravicini Bagliani, M. De Sanctis, A. Dimatteo, R. Ishak, R. Valentini

In the last years the development of innovative steels with a better combination of strength and ductility has been focused on the obtainment of multiphase microstructures containing austenite. Quenched and Partitioned (Q&P) steels, recently introduced as alternative to the conventional advanced high strength automotive steels or to medium carbon structural steels, are the subject of the present research.
In this study, the hydrogen embrittlement susceptibility of a medium carbon Q&P steel has been evaluated and compared to that of conventional Quench and Tempered steel with the same chemical composition and similar ultimate tensile stress (UTS). Slow Strain Rate Tensile (SSRT) tests performed on samples electrochemically charged at different hydrogen contents have shown that Q&P steels have a higher hydrogen embrittlement susceptibility than conventional ones.

INTRODUCTION

In the last decades, the development of multiphase steels has allowed to capitalize the best properties of each microstructural constituent in order to obtain good combination of mechanical strength and ductility. The former can be highly increased by martensite or bainite presence, while the latter can be controlled by the content of retained austenite.

In this scenario, the TRIP (TRansformation Induced Plasticity) steels [1-4], the MFCB (Martensite/Free Carbide Bainite) steels [5-8], the medium Manganese steels with ferritic/austenitic microstructure obtained by Austenite Reversion heat treatment (ART-annealing) [9-13], and the Q&P (Quenching and Partitioning) steels [14-18] with a mixed microstructure formed by low-carbon martensite

G. Lovicu, M. De Sanctis, R. Ishak, R. Valentini

Dipartimento di Ingegneria Civile e Industriale, Università di Pisa, Largo Lucio Lazzarino, 2 – 56122 Pisa, Italy; g.lovicu@diccism.unipi.it

E. Paravicini Bagliani

Tenaris Dalmine
Piazza Caduti 6 Luglio 1944, 1 - 24044 Dalmine, Italy

A. Dimatteo

TeCIP-PERCRO Scuola Superiore Sant'Anna – Via Alamanni, 56100 Ghezzano, Pisa, Italy

and retained austenite are some of the most promising steels.

All the abovementioned steels show retained austenite in their final microstructures, that is stabilized at low temperature by tailored chemical compositions and heat treatments. An appropriate heat treatment is necessary to allow the diffusion of austenite-stabilizing elements into the austenite phase (mainly Carbon and, in some cases, Manganese) and, consequently, its stabilization at room temperature. The choice of the chemical composition is essential in order to inhibit the carbide precipitation that is able to decrease the carbon content solubilized into austenite, thus avoiding its retention at room temperature. Silicon and aluminium are usually added for this purpose.

Among the most recently introduced multiphase steels, those obtained by Q&P process have been initially proposed as third generation of advanced automotive high strength steels or in substitution of conventional Quench and Tempered (Q&T) steels and they appear to be among the most interesting ones. For example, it is possible to reach Ultimate Tensile Strength (UTS) of about 1400 – 1500 MPa along with elongation at fracture of about 12 – 15 % [19,20]. The thermal treatment of a Q&P steel is composed by the following steps: (i) austenitization (partial or complete), (ii) interrupted quenching at a temperature between the martensite start (Ms) and the martensite finish (Mf) temperatures in order to obtain a mixed microstructure of martensite (or martensite/ferrite) and austenite, (iii) a holding at a temperature equal or higher than the quenching one (partitioning step) in

order to allow the carbon diffusion from martensite into austenite that induces the softening of the martensitic phase and the stabilization of the austenite; and (iv) a final fast cooling to room temperature in order to freeze the final microstructure. The carbon partitioning process from martensite to austenite has been extensively studied in the last years, both considering the microstructural evolution and its influence on the final mechanical properties [14,17,19,21]. Notwithstanding, the industrial production of these steels is very recent and limited (see for example [22]), above all for the difficulty to obtain a strict control of the interrupted quenching step.

One of the main limit to the use of high strength steels is related to their intrinsic susceptibility to hydrogen embrittlement. In fact, it is well known that, for steel belonging to a same class, hydrogen embrittlement susceptibility increases with the tensile strength [23,24]. Thus, the development of innovative ultra high strength steels needs a thoroughly analysis of their hydrogen embrittlement susceptibility. Moreover in case of multiphase steels containing retained austenite, this phase can play a fundamental role on the hydrogen embrittlement mechanism [25], because of its high toughness and on its very low hydrogen diffusivity able to limit the hydrogen ingress into the steel.

Usually, austenite particles dispersed in a martensitic or a ferritic matrix are treated as irreversible traps for hydrogen [22,26]. The presence of very small and homogeneously dispersed irreversible traps can play a beneficial role on hydrogen embrittlement, thanks to their ability to reduce the amount of diffusible hydrogen. It is well known, for example, the effect of fine vanadium carbides in decreasing the hydrogen embrittlement susceptibility of Cr-Mo steels (see, for example, [27]). In other cases the presence of precipitates can have a negative effect on the structural integrity of steels and on their hydrogen embrittlement resistance, as for example, in case of coarse grain boundaries precipitates [28].

The role of austenite as hydrogen trap is still under investigation. Although some studies show that austenite may represent a class of high energy hydrogen traps (such as [29]), other experimental works [30] performed on multiphase TRIP steels have shown the lack of high energy secondary peaks in TDA (Thermal Desorption Analysis) spectra. Recent studies have also shown a not negligible hydrogen embrittlement susceptibility of steels containing significant austenite volume fractions (as, for example, TRIP steels) [30-32]. Thus the field of hydrogen embrittlement of multiphase high strength steels needs more and thorough investigations.

The present paper is focused on the study of the hydrogen embrittlement susceptibility of a medium carbon Q&P steel, performed by SSRT (Slow Strain Rate Tensile) tests on samples charged at different hydrogen contents. A conventional Quench and Tempered steels with the same chemical composition and similar mechanical strength has been used as reference.

C	Si	Mn	Cr	Mo	other elements
0.23	1.5	1.4	2.2	0.9	Nb, Ni

Tab. 1 - Chemical composition of the selected material.

Tab. 1 - Composizione chimica degli acciai analizzati.

MATERIALS AND METHODS

The chemical composition of the selected material is reported in Table 1.

The heat was laboratory cast as ingot, hot rolled by a pilot mill in sheets of 8 mm thickness with a finish rolling temperature of about 1000 °C.

Subsequently, the sheets were thermally treated in order to produce two different steels: a Quenched and Partitioned steel (named "QP") and a conventional Quench and Tempered steel (named "QT").

The process parameters of Q&P cycle were optimized for the tested chemistry following methodologies described in previous works, through the determination of critical transformation temperatures and TTT diagrams by dilatometric techniques [19,21]. The Q&P heat treatment was performed in an industrial plant equipped with double salt baths. It consisted of the following steps: i) complete austenitization at 930 °C for 10 min; ii) quench in a salt bath at 235 – 245 °C in order to obtain about the 15 % of austenite in a martensite matrix; iii) partitioning in another salt bath at 450 °C for about 5 min in order to allow the carbon partitioning between martensite and austenite; iv) final cooling in water at room temperature.

The QT treatment, optimized in order to obtain similar mechanical strength, consisted of the following steps: i) complete austenitization at 930 °C for 10 min; ii) water quenching at room temperature; iii) tempering in furnace at 560 °C for 30 minutes; iv) final cooling in air.

Volume fractions of retained austenite have been measured by X-ray diffractometry, using the Rietveld method [33] for the spectra analysis.

The analysis of hydrogen trapping behaviour was performed by TDA using a hot extraction method on 25 mm x 15 mm x 2 mm coupons previously electrochemically charged. A heating rate of 5 °C/min was used. In order to explore different hydrogen activity conditions, coupons were hydrogenated by cathodic charging using both 0.1 N NaOH and 0.1 N H_2SO_4 water solutions containing recombination poisons (20 mg/l As_2O_3 and 5×10^{-4} M $NaAsO_2$, respectively).

The hydrogen embrittlement susceptibility was studied by SSRT tests performed on smooth samples having a rectangular section of 6 x 10 mm^2 and a gage length of 30 mm. Tensile tests were performed on a universal testing machine at a strain rate of about $(2 \div 4)\times10^{-5}$ s^{-1}. Samples had been previously hydrogenated in 0.1 N NaOH water solutions (with or without recombination poisons) using cathodic current densities ranging from 1 and 25 mA/cm^2 in order to induce different hydrogen concentrations on samples.
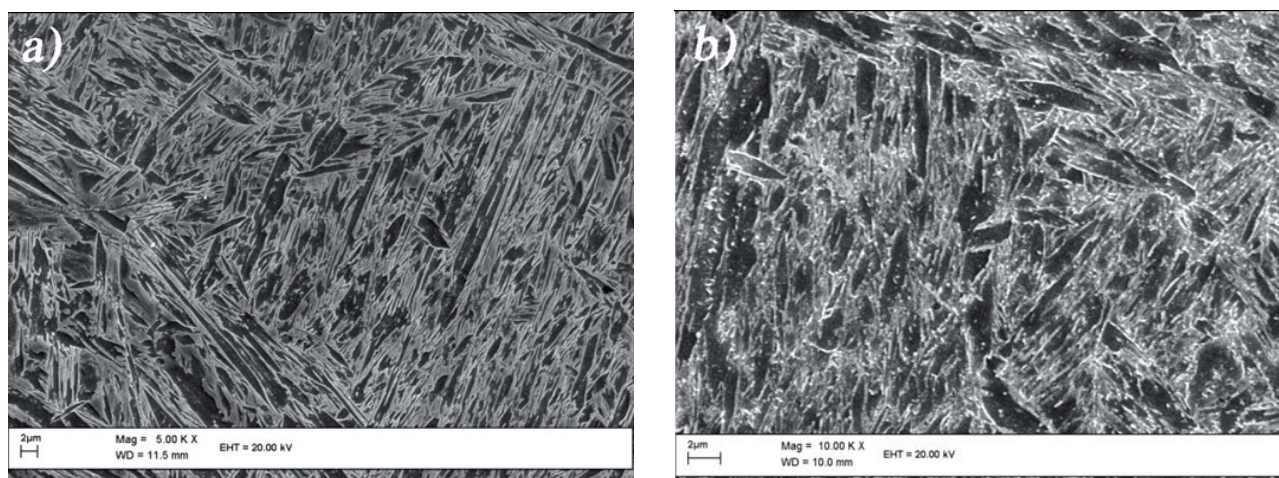
Fig. 1 - SEM micrographs of the tested steels. a) QP steel, b) QT steel.

Fig. 1 - Micrografie SEM dei campioni analizzati. a) acciaio QP, b) acciaio QT.

	Test	Material	Charging Solution	Cathodic current
Tab. 2 - Hydrogen charging conditions used in TDA tests. *Tab. 2 - Condizioni di caricamento utilizzate per le prove TDA.*	a	QT	NaOH (0.1 N) + As$_2$O$_3$ (20 mg/l)	2 mA/cm^2
	b	QP	NaOH (0.1 N) + As$_2$O$_3$ (20 mg/l)	2 mA/cm^2
	c	QP	H$_2$SO$_4$ (0.1 N) + NaAsO$_2$ (5·10^{-4} M)	2 mA/cm^2

At the end of tensile tests, one half of the fractured sample was used to determine the hydrogen content (by hot extraction method) while the other one was used to perform fractographic analysis using a Scanning Electron Microscope SEM (equipped with a microanalysis EDX system).

Hydrogen charging times for both the TDA and the SSRT tests were chosen in order to reach a uniform concentration on the sample sections (in particular they have been of at least 20 h and at least 40 h for TDA and SSRT tests, respectively).

RESULTS

Fig.1a shows the microstructure of the tested QP steel, observed by SEM after etching in 2 % Nital. The acicular microstructure is mainly composed by carbon depleted martensite laths, where, in some case, a slight presence of carbides can be noted, and areas that were not etched, that can be either retained austenite or not tempered high carbon martensite, formed in the final quench step.

The volume fraction of austenite was evaluated by means of X-ray diffraction. The percentage of retained austenite was equal to 17.5 ± 1.5% for QP steel and negligible (below the detection limit of the equipment (< 1 %)) for the QT steel. The Fig.1b shows a detail of the martensitic microstructure of QT steel.

Table 2 summarizes the hydrogen charging conditions used to perform TDA tests.

Both steels were tested in the same conditions, after
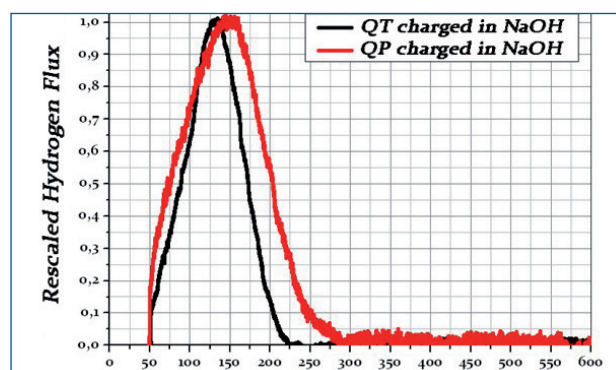
Fig. 2 - Comparison of TDA spectra of QP and QT steels hydrogenated in the same electrochemical condition (NaOH 0,1N + As$_2$O$_3$ 20 mg/l, 2mA/cm^2) and rescaled to the peak maximum value.

Fig. 2 - Confronto fra gli spettri TDA (condotti a 5°C/min) degli acciai QT e QP idrogenati nelle stesse condizioni elettrochimiche (NaOH 0,1N + As$_2$O$_3$ 20 mg/l, 2 mA/cm^2) e normalizzati al valore del massimo.

hydrogenation in a 0.1 N NaOH water solution containing As$_2$O$_3$ (20 mg/l). Moreover, other tests were performed on QP steel hydrogenated in a 0.1 N H$_2$SO$_4$ water solution containing NaAsO$_2$ (5×10^{-4} M), in order to highlight the possible influence of the hydrogen activity on the hydrogen distribution in the trapping sites.

TDA spectra of QP and QT steels tested in the a and b conditions (specified in Table 2) are shown in Fig.2. In order to have a better comparison of position and width of
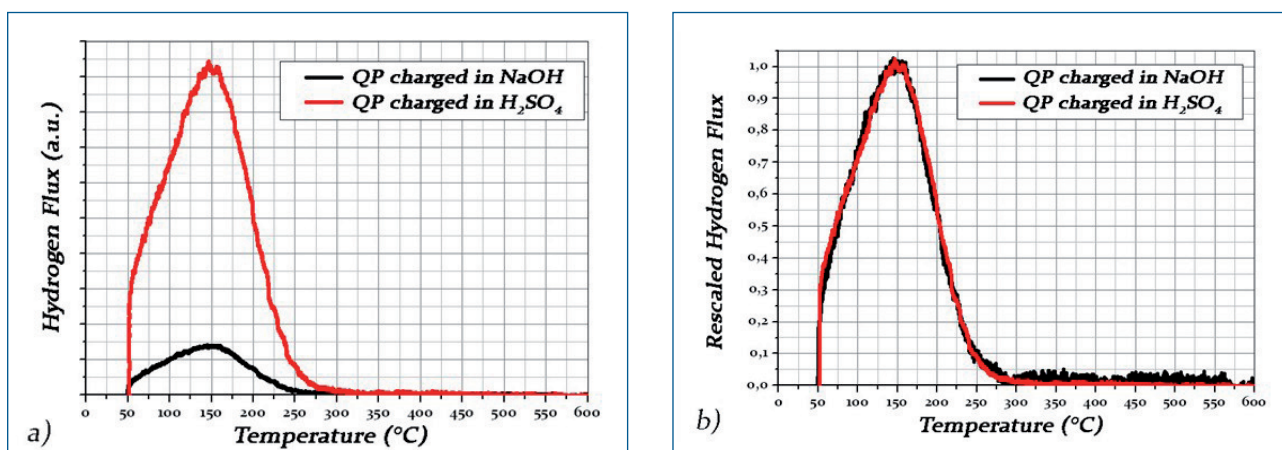
Fig.3: **a) Comparison of TDA spectra of QP steels hydrogenated in NaOH and H2SO4 aqueous solutions; b) TDA spectra of Fig.3a rescaled at the peak maximum value.**

a) Confronto fra gli spettri TDA (condotti a 5°C/min) dell'acciaio QP idrogenato in soda e in acido solforico; b) stessi spettri TDA normalizzati al valore del massimo.
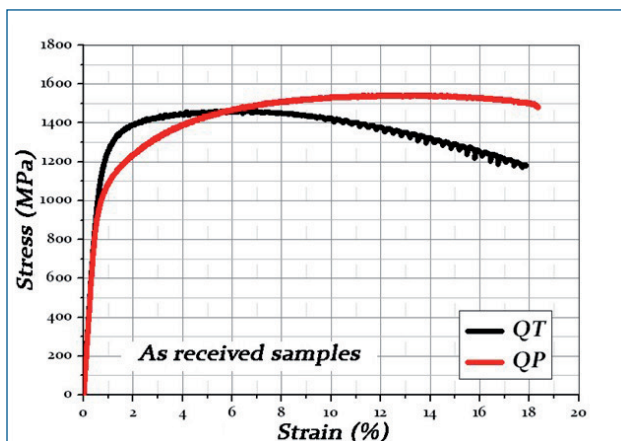
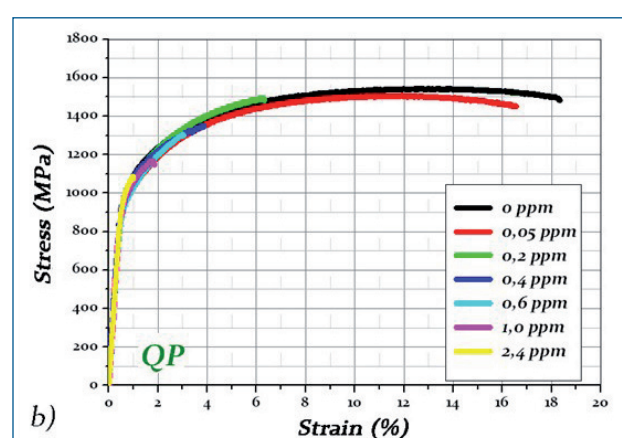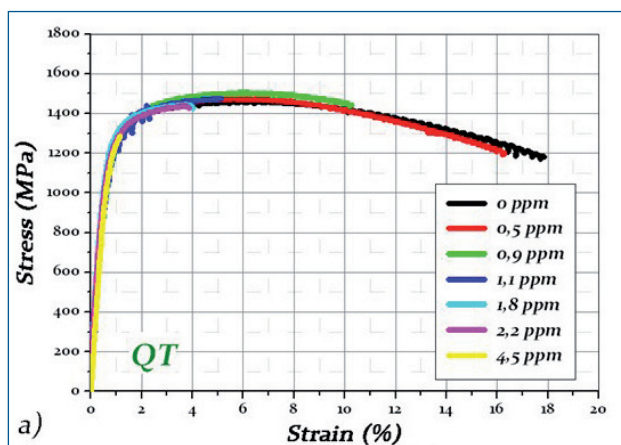**Fig.4 - Stress-strain curves of QP and QT steels in as-received condition.**

Fig. 4 - *Curve sforzo-deformazione ottenute su campioni tal quale degli acciai testati.*

desorption peaks, spectra have been rescaled to the peak maximum value.

It can be observed that in both steels the hydrogen desorption takes place in a single peak, positioned in the range of temperatures that is typical of low energy traps (such as dislocations or grain boundaries). Moreover, the desorption peak of QP Steel is at temperatures slightly higher and it is slightly wider than that of QT steel.
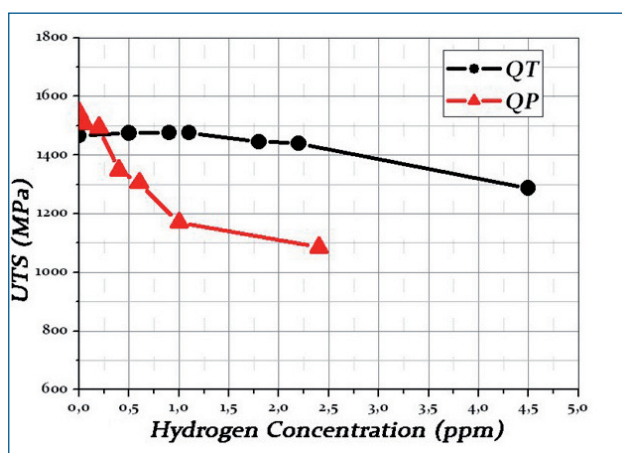
In Fig.3a the TDA curves obtained on QP steel for different hydrogenation conditions (tests *b* and *c* of Table 2) are shown.

Even after hydrogenation in sulfuric acid, the TDA spectra do not show any secondary peak at higher temperature (fig. 3). The different hydrogen activity related to the use of an acidic solution leads to a higher hydrogen concentration, and thus to a greater quantity of desorbed hydrogen. However there are neither variations in the position of the peak nor in its shape. In fact, rescaled spectra show the same shape, and the only difference is a scale factor.

Results of these tests demonstrate the absence of high

Fig. 5 - Stress-strain curves of QT (a) e QP (b) at different hydrogen concentrations.

Fig. 5 -*Curve sforzo-deformazione ottenute su campioni QT (a) e QP (b) con diverse concentrazioni di idrogeno.*

Fig. 6 - Ultimate Tensile Strength (UTS) of the tested steels as function of the hydrogen concentration.

Fig. 6 - Carico di rottura (UTS) degli acciai testati in funzione della concentrazione d'idrogeno.

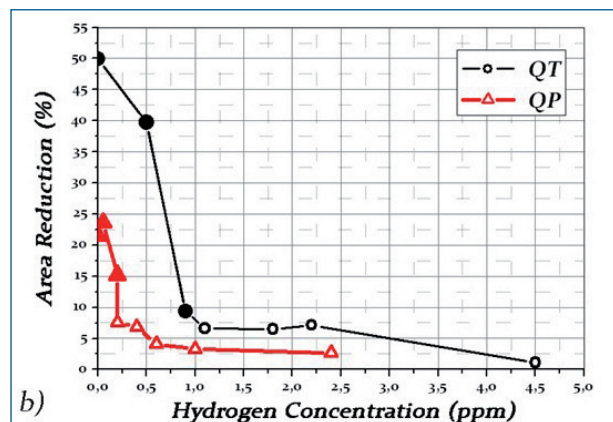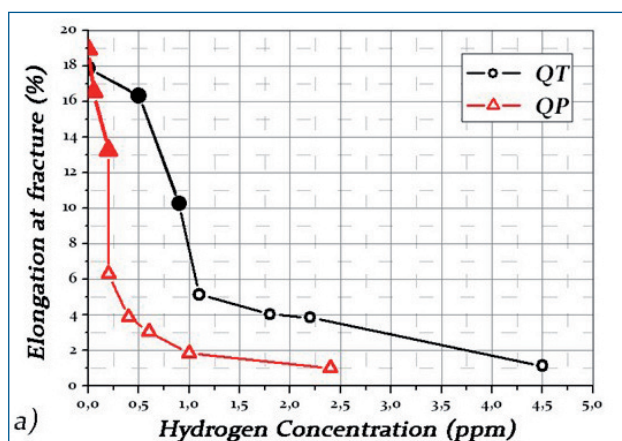In Fig.5 the stress-strain curves of the analysed steels charged at different hydrogen contents are shown.

The principal effect of hydrogen is to shorten the stress-strain curves, reducing the ductility of the steel and the elongation to fracture as the amount of hydrogen increases.

The analysis of the susceptibility to hydrogen embrittlement and the determination of the critical concentration of the two examined steels were carried out through the study of variation of strength and ductility parameters as function of the hydrogen concentration (see Fig.6 and 7) along with fractographic analyses of specimens subjected to tensile tests.

Fig. 6 shows the UTS values as a function of the hydrogen concentration for the analyzed steels. QP steel exhibits a sharp decrease at values of hydrogen concentrations less than 0.5 ppm. For higher concentrations (greater than 2 ppm) the UTS is about 30% lower than the as received samples. The QT steel shows a smoother curve, without a marked UTS drop even at high concentrations. The maximum recorded reduction of tensile strength is about 10%.

This different behavior may be partially attributed to the different form of the stress-strain curves of the two tested steels. The QP steels show, in fact, a larger work hardening and a higher uniform elongation, whereas, for the QT steels, the uniform elongation is lower and the shortening of the stress-strain curve due to the presence of hydrogen does not change significantly its UTS value.

However, the proposed explanation can not clarify the differences in the embrittlement curves calculated from ductility parameters (elongation and reduction of area). Also in this case, the curves show remarkable differences between the two steels, with a much more sudden drop in both parameters for the QP steel than the QT one (Fig. 7). It is interesting to note the difference, between the QT and QP steels, of the area reduction values of the not hydrogenated samples. This difference is imputable to the different shape of their engineering tensile curves. In the

energy traps in both examined materials. The effect of austenite on the hydrogen trapping, if present, is limited to a slight enlargement and shift of the peak towards higher temperature.

In Fig.4 the stress-strain curves of the QT and QP steels are shown in as-received conditions, with a residual hydrogen virtually equal to zero (a hydrogen content less than 0.1 ppm was measured).

The QP steel is characterized by lower yield stress and higher tensile strength than the QT one. This is because the presence of austenite phase in QP steel increases the strain hardening of the steel. Moreover, the two materials exhibit a significant difference in the value of uniform elongation: about 5 % for the QT steel and about 15 % for QP steel. The high value of uniform elongation makes the QP steel particularly suited to be formed.

Fig. 7 - Uniform elongation (a) and area reduction (b) of the steels tested at different hydrogen content. Open symbols indicate specimens where large inclusions have been revealed on the fracture surface.

Fig. 7 - Allungamento a rottura (a) e riduzione d'area (b) degli acciai testati in funzione della concentrazione d'idrogeno. I simboli vuoti si riferiscono ai campioni per i quali sono state rilevate macroinclusioni nella superficie di frattura.
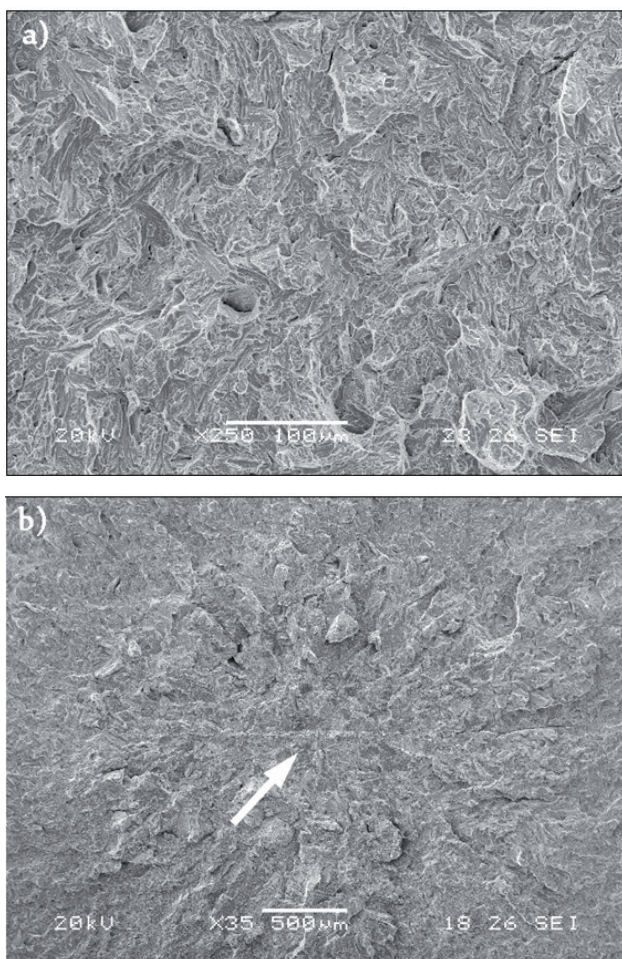
Fig. 8 - a) QP steel with hydrogen concentration equal to 0.5 ppm. Fractograph from the core of the sample, b) Presence of a large inclusion (indicated by the arrow) in QP specimen with hydrogen concentration equal to 0.5ppm. Ridges orientation indicates the crack initiation site at inclusion.

Fig. 8 - a) Acciaio QP con concentrazione di idrogeno pari a 0,5 ppm. Zona a cuore, b) Innesco della frattura in corrispondenza di un'inclusione (indicata dalla freccia) in un campione QP idrogenato con 0,5 ppm.

case of the QP steel, the deformation is mainly related to the uniform elongation. On the other hand QT steel have a total elongation driven by the post-necking deformation. Thus, although the values of total elongation are very similar (at least in not hydrogenated specimens), the values of area reduction differ considerably, being much lower for the QP steel.

The fractographic analyses have shown some typical characteristics of hydrogen assisted fractures as transgranular quasi-cleavage brittle fracture mode (Fig.8a) and the presence of secondary cracks. Moreover they have shown that, in several samples, the fracture initiation point corresponded with the presence of large alumina inclusions, highlighted by the orientation of ridges (see Fig. 8b). The effect of hydrogen accumulation in the inclusions/matrix

interface areas, along with their sharp tip (particularly disadvantageous in terms of stress intensification factor), make large inclusions able to significantly increase the hydrogen embrittlement susceptibility of steels, especially in case of ultra-high-strength steels.

DISCUSSION

In order to explain the experimental results obtained by tensile tests and fractographic analysis it is good to pay attention to some factors that relate the decrease of ductility parameters to the concentration of absorbed hydrogen and to the presence of large inclusions in the fracture surface. From data reported in Fig.7 two main considerations can be done:

A. for each investigated steel, only specimens charged at hydrogen concentrations over a threshold value show the presence of large inclusions in the fracture surface;
B. the decrease of ultimate elongation and area reduction is already evident in samples that do not show the presence of large inclusions in the fracture surface.

Considering that all the tested samples come from the same laboratory heat, it is presumable that all specimens were affected by the presence of the same type of inclusions. Moreover, from point A, it is evident that these inclusions are able to activate the crack formation process only when a certain critical threshold of hydrogen concentration is reached. Results show that this threshold is very well defined. All the samples with hydrogen concentrations lower than the threshold value have not shown any inclusions on the fracture surface, whereas all samples with higher concentrations have shown them clearly. Finally, the threshold value is material dependent. QP steel samples have shown area reduction values significantly lower than those of QT steel ones, along with a lower hydrogen concentration threshold for the activation of inclusions in the fracture process (0.2 *vs* 1.0 ppm).

From point B it can be noted that the embrittlement effect of hydrogen is highlighted even in samples that have not shown large inclusions in their fracture surface. In fact, the decrease of ductility properties as a function of hydrogen concentration is evident already at very low concentration values (see Fig. 7), ie for those specimens characterized by the absence of inclusions in the fracture surface. Obviously, the presence of coarse inclusions contributes to a further reduction in the sample ductility, and, in fact, at the same hydrogen concentration, the specimens with inclusions have shown smaller reductions of area (see, for example, the QP specimens with $C_H = 0.2$ ppm). Thus, from the analysis of SSRT results, a greater susceptibility of the QP steel than the QT one of same chemical composition and similar tensile strength can be highlighted, even without considering the large inclusions effects. This could be reasonably attributed to their different microstructures, and in particular to their main difference, ie the presence of austenite in QP steel.

Austenite do not always play a positive role in the

behaviour of hydrogen embrittlement. In particular, the tendency of this phase to transform into martensite during deformation (TRIP effect) can increase embrittlement susceptibility [30, 34]. The austenitic phase, thanks to its high hydrogen solubility, can be characterized by hydrogen concentrations considerably higher than those of the surrounding martensitic matrix. These concentrations are maintained unchanged in the martensite resulting from the deformation induced transformation of austenite, resulting in a high probability of micro-cracks formation, that can greatly accelerate the final fracture process.

CONCLUSIONS

From the achieved results, the following conclusions can be summarized:

1. The Q&T and Q&P steels, at the same strength level condition, have shown very similar thermal desorption spectra. Despite the presence of austenite in the QP microstructure high temperature peaks have not been revealed.

2. QP steel has shown a lower resistance to hydrogen embrittlement that has been highlighted by a greater and early decrease of mechanical strength and ductility in respect to the hydrogen content. The analysis of the influence of large inclusions detected in the samples has showed that this behavior is valid regardless of their presence.

3. It is reasonable to assume that the tendency of the austenitic phase to transform into martensite during plastic deformation (TRIP effect), along with the high concentrations that hydrogen can reach within this phase, can play an important role in the crack initiation step at the transformed martensite areas, that, in turn, can drive the final cracking process.

REFERENCES

1. J. Mahieu, D. Van Dooren, L. Barbé, B.C. De Cooman, Proceedings of the Int. Conf. On TRIP-aided high strength ferrous alloys (ed. by De Cooman), Ghent, (B), June 19-21, (2002), pp. 159-164.
2. A.N. Vasilakos, J. Ohlert, K. Giasla, G.N. Heidemenopoulos, W. Bleck, Proceedings of the Int. Conf. On TRIP-aided high strength ferrous alloys (ed. by De Cooman), Ghent, (B), June 19-21, (2002), pp. 277-280.
3. M. De Myer, D. Vandershueren, B.C. De Cooman, ISIJ (1999), vol. 39 n.8, pp.819-828.
4. A. Zarei Hanzaki, P.D. Hodgson, S. Yue: ISIJ Int., (1995), vol.35, n.1, pp. 79-85.
5. S. Sharma, S. Sangal, K. Mondal, Metallurgical and Materials Transactions A, (2011), Vol. 42^a, pp. 3921-3933.
6. C. Garcia-Mateo and F.G. Caballero: ISIJ Int., (2005), vol. 45, pp. 1736–40.
7. H.K.D.H. Bhadeshia: Mater. Sci. Forum, (2005), vols. 500–501, pp. 63–74.
8. D. Liu, B. Bai, H. Fang, W. Zhang, J.n Gu, K. Chang, Materials Science and Engineering A (2004) vol.371, pp. 40–44.
9. H.N. Han, C.S. Oh, G. Kim, O. Kwon, Mater. Sci. Eng. A 499 (2009) 462.
10. J. Shi, X. Sun, M. Wang, W. Hui, H. Dong and W. Cao, Scripta Materialia (2010) vol.63, pp.815-818.
11. H. Luo, J. Shi, C. Wang, W. Cao, X. Sun, H. Dong, Acta Materialia (2011) vol.59, pp. 4002-4014.
12. C. Wang, J. Shi, C. Y. Wang, W. J. Hui, M. Q. Wang, H. Dong and W. Q. Cao, ISIJ International, (2011), Vol. 51 No. 4, pp. 651-656.
13. W.Q. Cao, C. Wang, J. Shi, M.Q. Wang, W.J. Hui, H. Dong, Materials Science and Engineering A (2011) vol.528, pp.6661- 6666.
14. J. Speer, D.K. Matlock, B.C. De Cooman, and J.G. Schroth: Acta Mater., (2003), vol. 51, pp. 611–622.
15. D.K. Matlock, V.E. Brautigam, and J.G. Speer: Mater. Sci. Forum, (2003), vols. 426–432, pp. 1089–1094.
16. J. G. Speer, F. C. Rizzo Assunção, D. K. Matlock, D. V. Edmonds, Materials Research, (2005) Vol. 8, No. 4, 417-423.
17. A.J. Clarke, J.G. Speer, M.K. Miller, R.E. Hackenberg, D.V. Edmonds, D.K. Matlock, F.C. Rizzo, K.D. Clarke, E. De Moor, Acta Materialia (2008) vol. 56, pp. 16–22.
18. E. Paravicini Bagliani, E. Anelli, M. Boniardi, Materials Science Forum, (2012) Vols.706-709, pp. 2234-2239.
19. M.J. Santofimia, L. Zhao, R. Petrov, C. Kwakernaak, W.G. Sloof, J. Sietsma, Acta Materialia (2011) 59, 6059-6068.
20. 130E. De Moor, J.G. Speer, D.K. Matlock, J.H. Kwak, S.-B. Lee, ISIJ International, (2011) Vol. 51, pp.137-144.
21 E. Paravicini Bagliani, M.J. Santofimia, L... Zhao, J. Sietsma, E. Anelli., Materials Science & EngineeringA (2012), http://dx.doi.org/10.1016/j.msea.2012.08.
22. L. Wang and W. Feng, Advanced Steels, Y. Weng et al. (eds.), Springer-Verlag, Berlin 2011.
23. R.A. Oriani, J.P. Hirth, M. Smialowski: Hydrogen degradation of Ferrous Alloys, Noyes Publications, Park Ridge, NJ, USA, 1985.
24 ASM Materials Handbook, Metals Handbook, 9th edn., vol. 13, Corrosion, ASM International, Materials Park,

OH (1987), p.330.

25. J. L. Gu, K. D. Chang, H. S. Fang, B. Z. Bai, ISIJ International, (2002), Vol. 42 No. 12, pp. 1560–1564.

26. C. Gesnouin, A. Hazarabedian, P. Bruzzoni, J. Ovejero-Garcıa, P. Bilmes, C. Llorente, Corrosion Science (2004) vol.46, n.7, pp. 1633-1647.

27. H. Shimazu et al., Proceedings of the ASME 2012 Pressure Vessels & Piping Conference, (2012)

28. Michler, Balogh, International Journal of Hydrogen energy (2010) vol.35, pp. 9746-9754.

29. Y.D. Park, I.S. Maroef, A. Landau, D.L. Olson: Welding Research, (2002), pp.27-35.

30. J. H. Ryu, Y. S. Chun, C. S. Lee, H.K.D.H. Bhadeshia, D. W. Suh: Acta Materialia, 2012, Vol.60, n. 10, pp.4085-4092.

31. J. Sojka, V. Vodarek, I. Schindler, C. Ly, M. Jerome, P. Vanova, N. Ruscassier, A. Wenglorzova, Corrosion Science (2011) vol. 53, pp. 2575–2581.

32. J.A. Ronevich, B.C. De Cooman, J.G. Speer, E. De Moor, D.K. Matlock, Metallurgical and Materials Transactions A, (2012), Vol.43A, pp. 2293-2301.

33. D.L. Bish, S.A. Howard, J. Appl.Cryst. (1988), vol.21 pp. 86-91.

34. G. Lovicu, M. Bottazzi, F. D'aiuto, M. De Sanctis, A. Dimatteo, C. Santus, R. Valentini: Metallurgical and Materials Transactions A, (2012), Vol.43A, pp. 4075-4087.

Infragilimento da idrogeno di acciai Q&P

Parole chiave: Acciaio - Trattamenti termici - Caratterizzazione materiali

Lo sviluppo di acciai con una sempre migliore combinazione di resistenza e duttilità ha puntato recentemente alla realizzazione di microstrutture multifase contenenti austenite. Fra questi materiali si possono ricordare gli acciai Q&P (Quench and Partitioning), che, recentemente studiati, potrebbero sostituire gli acciai convenzionali in diversi campi applicativi, quali l'automobilistico negli acciai ad alta stampabilità e quello della componentistica meccanica al posto degli acciai a medio carbonio da trattamento termico.

Il processo di "Quenching and Partitioning" prevede austenitizzazione (completa o parziale), tempra interrotta ad una temperatura compresa fra la temperatura di martensite start (Ms) e quella di martensite finish (Mf) in modo da ottenere una microstruttura mista di martensite (o martensite/ferrite) ed austenite residua e un successivo trattamento ad una temperatura di *partizionamento* (eguale o superiore a quella di interruzione della tempra) in modo da permettere la diffusione del carbonio dalla martensite all'austenite residua con conseguente addolcimento della prima e stabilizzazione della seconda fase. La chimica di questi acciai è stata ottimizzata principalmente al fine di permettere la formazione di una buona quantità di austenite a temperatura ambiente. In particolare si agisce aumentando il contenuto di silicio per evitare la formazione di carburi durante il processo di ridistribuzione del carbonio, facilitando l'arricchimento di carbonio dell'austenite, e quindi la sua stabilità.

Il presente lavoro analizza la suscettibilità ad infragilimento da idrogeno di acciai Q&P a medio tenore di carbonio in confronto con quella dei corrispondenti convenzionali "quench and tempered".

Lo studio ha riguardato un acciaio a medio carbonio (0.22%) ed alto Si (1.5%), legato con Mn, Cr, Ni e Mo.

Da una stessa colata di laboratorio sono state realizzate due tipologie di materiali con carichi di rottura confrontabili (1400-1500 MPa):

- la prima con un convenzionale ciclo di tempra e rinvenimento;

- la seconda con cicli di "quenching and partitioning", al fine di ottenere una microstruttura di martensite con significative frazioni volumetriche di austenite residua.

L'interazione fra l'idrogeno e i materiali in esame è stata studiata a mezzo di prove di desorbimento termico a temperatura programmata. La suscettibilità ad infragilimento da idrogeno è stata inoltre analizzata tramite prove di trazione a bassa velocità di deformazione (SSRT) su provini idrogenati a diverse concentrazioni.

Le prove di desorbimento termico non hanno evidenziato la presenza di trappole ad alta energia in entrambi i materiali. Le prove SSRT hanno indicato una minore resistenza all'infragilimento da idrogeno per gli acciai contenenti austenite residua che si è manifestata con una più marcata decrescita delle proprietà di resistenza e duttilità associata ad una concentrazione critica di idrogeno inferiore. L'analisi frattografica dei provini di trazione ha evidenziato la presenza di inclusioni di allumina che hanno giocato un ruolo attivo nel processo di frattura dei materiali testati. Le inclusioni risultano visibili come siti di innesco della frattura solo per concentrazioni d'idrogeno superiori ad un valore di soglia. La maggiore suscettibilità all'infragilimento da idrogeno degli acciai Q&P si è manifestata con una soglia di attivazione delle inclusioni minore per questi acciai rispetto ai corrispettivi convenzionali Q&T. Dai risultati ottenuti in questo studio, è ragionevole concludere che la complessa microstruttura degli acciai Q&P giochi sfavorevolmente nelle dinamiche di infragilimento da idrogeno. In particolare, la trasformazione dell'austenite durante la deformazione (effetto TRIP) in una martensite ricca di carbonio e di idrogeno può facilitare notevolmente il processo di frattura del materiale.